Innovative High-Pressure Water Scrubber for biogas upgrading at farm-scale using vacuum for water regeneration

Eliot Wantz, Mathis Lemonnier, David Benizri, Nicolas Dietrich, Gilles Hébrard

Innovative High-Pressure Water Scrubber for biogas upgrading at farm-scale using vacuum for water regeneration

Eliot Wantz[1], Mathis Lemonnier[1], David Benizri[2], Nicolas Dietrich[1], Gilles Hébrard[1,*]

[1] *TBI, Université de Toulouse, CNRS, INRAE, INSA, Toulouse, France*

[2] *Epurtek, SAS, 81 Chemin de Mange-Pommes, 31520 Ramonville-Saint-Agne, France*

*Corresponding author: gilles.hebrard@insa-toulouse.fr (G. Hébrard)

Highlights

- Rough vacuum (0.8 to 0.2 bar) is applied to enhance water regeneration
- A full-scale prototype is set up and tested on a farm anaerobic digester
- Vacuum enhances water regeneration (+10 % CH_4 purity) and methane recovery (+10 %)
- Anisotropic packing allows to reach high CH_4 purity over 97 % for gas grid injection
- Energy efficiency is 91 % for an electrical consumption of 0.38 kWh/Nm^3

Abstract

Biogas upgrading is becoming essential in the valorization path for biogas. Biomethane from anaerobic digestion is identified to be one of the main resources to decarbonize the energy requirement. However, small-scale (especially farm-scale) applications suffer from a lack of implementation worldwide, mainly limited by the cost of the upgrading process. As one of the most used technologies, High Pressure Water Scrubbing presents a great margin for improvement. The most expansive items in this technology remain the packing column used for absorption and the stripping column used for water regeneration. In this work, the stripping column is replaced by a flash tank submitted to a rough vacuum (up to 0.2 bar in absolute pressure) associated to a static mixer to promote the gas desorption and thus the complete regeneration of the water. The implementation of an anisotropic packing, with properties evolving with the height of the column and adapted to the reduction of the gas flowrate due to absorption, is also investigated in order to reduce the size of the absorption column. A full-scale prototype was developed and implemented on a farm anaerobic digester. The range of application is from 20 to 40 Nm^3/h of raw

biogas. These field experiments associated to a complete description of the gas fluxes allowed to characterize the device in terms of carbon dioxide absorption efficiency, biomethane purity and methane recovery. Influences of six parameters (absorption pressure, desorption pressure, temperature, water flowrate, biogas flowrate, column height) were elucidated regarding those performances. Results highlight the great improvement of the water regeneration conducted under rough vacuum. From 0.8 to 0.2 bar in absolute pressure, the biomethane purity increased by 10 %, the carbon dioxide elimination rate by 14 %, and the methane recovery by 19 %. With an increase in the packing height using an anisotropic configuration (modification of the packing properties with the column height) suited to the gas flowrate decrease into the column, a biomethane purity over 97 % was obtained. The energy consumption associated was measured at 0.8 kWh/Nm^3 of raw biogas but can be reduced to 0.3 kWh/Nm^3. The overall energy efficiency for biogas upgrading can reach up to 91 %. These results could pave the way for gas grid injection and vehicle fuel applications for small-scale anaerobic digestion.

Keywords

Biogas Upgrading, High Pressure Water Scrubbing, Small-Scale Anaerobic Digestion, Biomethane, Packing Material, Energy Efficiency

1 Introduction

Biogas is a promising energy resource for the mitigation of industrial impacts [1]. It is more and more integrated in the carbon-neutral long-term vision for the energy mix in several policy frameworks. The valorization path of biogas is mostly divided in Combined Heat and Power generation (CHP) and biogas upgrading (for gas grid injection or biofuel utilization), as illustrated in Figure 1. The latter is gaining increasing interest on the market with more and more incentive policies [2]. Indeed, CHP costs remain high in comparison to other renewable electricity productions (such as solar photovoltaics or onshore winds), and its valorization efficiency strongly depends on the heat valorization that is very difficult to achieve, especially in rural areas [3]. As available organic matter for anaerobic digestion is mostly located in rural areas, economic viability is nowadays very difficult to attain for these valorization paths, and biogas upgrading could be a possible solution to overcome this viability issue. However, in rural areas, small-scale anaerobic digestion is better suited to the area of distribution, and the associated cost of biogas upgrading is still too high to reach viability [4]. The development of farm-scale anaerobic digestion is therefore, in many countries worldwide, highly investigated but still limited to the development of

technologies suited to small-scale plants [2,5,6]. Attention should therefore be addressed to the development of cost-efficient solutions for biogas upgrading at small-scale.

A wide diversity of upgrading technologies are developed and presented in literature. The most common technologies are membrane based, physical absorption, chemical absorption, adsorption and cryogenic separation,

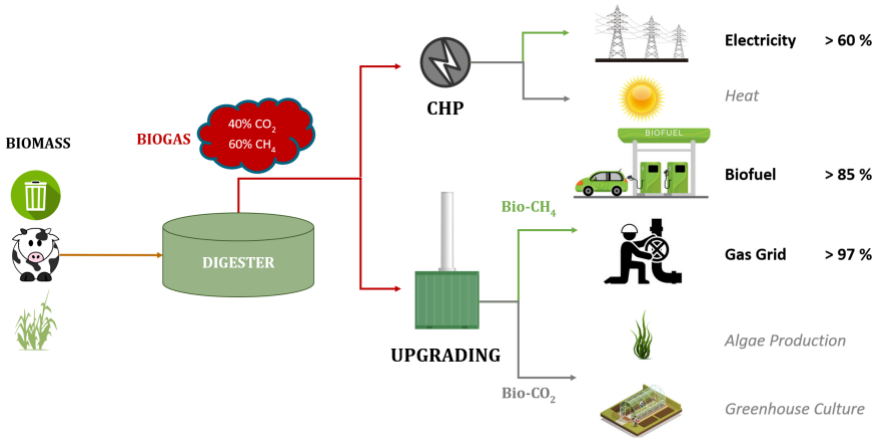

Figure 1: Farm-scale anaerobic digestion plant.

as compared in several reviews [7–9]. Other emerging technologies (*in situ* or *ex situ*) are currently under development [10–12]. *In situ* techniques are conducted directly in the digester to convert carbon dioxide to methane e.g. in the case of hydrogenotrophic methanogenesis (using hydrogen input from eletctrolysis), or with electromethanogenesis [13,14]. *Ex situ* techniques are based either on the separation of carbon dioxide from the methane or on the conversion of carbon dioxide (to methane or a product that can be easily separated). For the separation, emerging techniques use innovative materials, such as natural clay, metal organic frameworks, wood ash, or ionic liquids [15–17]. For the conversion, photosynthetic removal of carbon dioxide using microalgae or methanation can be set up [18–21]. In the sake of a rapid and universal deployment for small-scale anaerobic digestion, these emerging techniques suffer from the availability of materials used or from the more complicated process integration required. Therefore, the enhancement of more conventional technics could be more adapted to the use of anaerobic digestion at small-scale in the nearest future. Among the most conventional techniques, High Pressure Water Scrubbing (HPWS) is one of the major technologies implemented for biogas upgrading. It appears that HPWS presents several advantages for the implementation at small-scale in rural environments, as discussed by Kapoor et al. (2021) and Sahota et al. (2018). Kapoor et al. (2021) [22] reviewed most recent works conducted on biogas upgrading with HPWS. The main conclusion is that HPWS is a complex device as many parameters should be considered, such as absorption pressure, gas to liquid flowrate and temperature. Moreover, these parameters are dependent on the column design, that affects the mass transfer efficiency. One parameter currently

missing when considering HPWS is the efficiency of the regeneration. Large scale plants use air stripping to regenerate the water. When air stripping is conducted, water is supposed to be fully regenerated. Yet, air stripping is associated to high investment and operating costs. Also, air stripping causes technical issues at long term as oxygen dissolves in the water, leading to bacterial growth and clogging on the packing. Oxygen and nitrogen dissolution finally end in biomethane that can cause impurity issues [23]. Besides, air stripping does not permit to valorize carbon dioxide, as it is diluted in the air stream and released into the atmosphere.

The literature is very scarce concerning experimental data about biogas upgrading with HPWS [24]. To the authors' knowledge, the work of Rasi et al. (2008) and Läntela et al. (2012) [25,26], Kapoor et al. (2017) [27,28] and Benizri et al. (2019) [29] present interesting results. Rasi et al. (2008) [25] used a height-to-diameter ratio of the column of 3:1 instead of the more conventional 20:1 [22] but with a higher absorption pressure (up to 30 bars instead of 10 bars). The biogas was from landfill and therefore contained a high amount of air. Nevertheless, this set-up results in an interesting methane purity of over 90 %. However, the water was not recirculated in a closed loop and methane losses were not evaluated. In Läntela et al. (2012) [26], the same set-up was used but a slight depression (around 0.7 bars in absolute pressure) was applied for water regeneration and the device was run on a closed water loop. As biogas composition presents a lot of variabilities, it was difficult to establish clear trends but a methane purity of 90 % was also obtained, which is similar to the configuration without water recirculation, meaning that the desorption is quite efficient. The energy consumption for this set-up was between 0.43 and 0.55 kWh/Nm^3 of raw biogas. Methane losses for this configuration were not determined though, and the influence of the desorption pressure were not evaluated. In Kapoor et al. (2017), authors focused on methane recovery by implementing an intermediate flash pressure between the absorption column and the regeneration unit to recover methane that had solubilized in the water. The biogas used is from de-oiled seed cake. The set up is more conventional, with a height-to-diameter ratio of 20:1 and absorption pressure around 10 bars. The gas-to-liquid ratio was around 5, and the methane purity obtained was around 94 %. In Benizri et al. (2019), the authors used a lower height-to-diameter ratio of 10:1 for the upgrading of 40 Nm^3/h of biogas from a farm plant at 8 bars (gas-to-liquid ratio of 5). The methane purity was close to 80 % with a methane recovery of 94 %. In this case, the water was entirely recirculated after desorption at atmospheric pressure. The three authors seek to develop biogas upgrading for small-scale applications by using innovative configurations, whether it is for the absorption or for the desorption. But there is still margin for improvement as in most countries, gas injection standards are around 96 to 97 %, requiring more efficient absorption processes. None of these studies actually focused on the efficiency of the water regeneration.

In a recently published work (Wantz et al. (2022) [30]), a modelling approach based on rate-based modeling for biogas upgrading considering concomitant absorption of methane and carbon dioxide was proposed. The results suggest that desorption under vacuum could be beneficial for biogas upgrading. Indeed, vacuum enables to reach targeted methane purity, but it also helps lowering the global energy requirement of the set-up, as an optimum can be reached by striking at a suitable set of pressure, gas to liquid ratio, and desorption pressure. A first experimental attempt was made by Jin et al. (2021) [31] to prove the feasibility of vacuum to enhance water regeneration. The authors used a synthetic biogas containing carbon dioxide in nitrogen. The set-up was a lab-scale device with a stripping column for water regeneration with air injection. The results show that carbon dioxide concentration in the water leaving the stripping column was much lower when decreasing the pressure to vacuum up to 0.1 bar, and that the air flowrate could be reduced accordingly to obtain similar performances. Also, it was established in Wantz et al. (2022) that a significant reduction of the flowrate occurs between the biogas inlet and the biomethane leaving the absorption column [30]. No studies were found considering the influence of this specificity on the mass transfer and the absorption efficiency for biogas upgrading. But as presented for example in Gładyszewski et al. (2021) [32], in the case of a rotating packed bed, the modification of gas and liquid loads can affect the transfer efficiency. The authors evaluate the influence of the implementation of an anisotropic packing, with properties of the packing evolving with the radius to be suited to the gas and liquid distribution. The results show an improvement in the transfer efficiency under this configuration. This kind of layout could be effectively applied in the case of biogas upgrading as it is also submitted to variations in gas loads.

This work aims at developing a full scale HPWS adapted to biogas upgrading for small-scale anaerobic digestion. Innovations are implemented to reduce the cost associated to the upgrading of biogas to reach financial viability at farm scale. The primary objective is to investigate the influence of vacuum on the regeneration of the water and to highlight the impact on the upgrading performances. Also, an anisotropic packing layout is investigated, to evaluate the feasibility in the case of packing column and to assess the performances on biogas upgrading. Other parameters such as absorption pressure, water temperature, and water flowrate were studied to complete the literature database. Finally, energy consumptions were analyzed to evaluate the set-up.

2 Experimental Methods

2.1 Experimental set up

The process developed in this work is called Epurogaz. It is a HPWS designed to upgrade a biogas flowrate ranging from 20 to 40 Nm^3/h. A simplified description of the setup is presented in Figure 2.

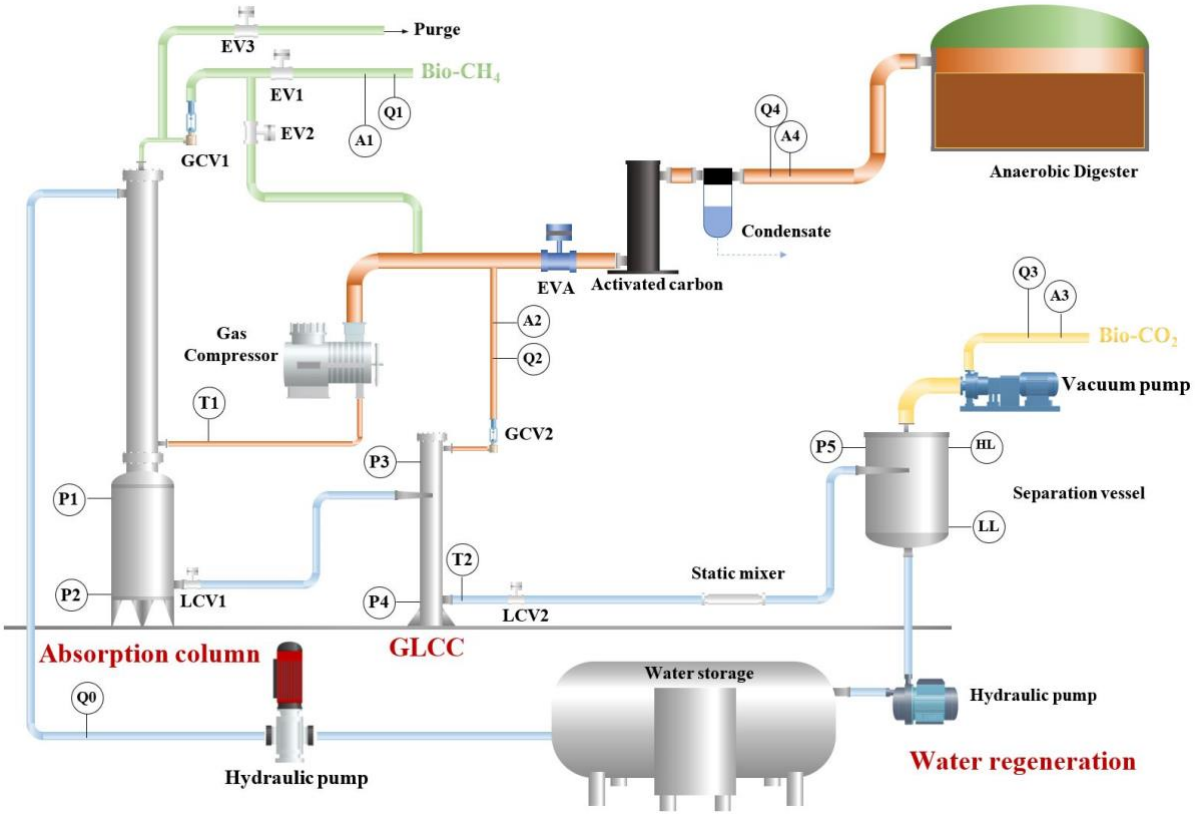

Figure 2: Simplified description of the biogas upgrading process.

It is composed of 3 main parts: the absorption column, the GLCC, and the water regeneration unit (composed of a static mixer, a vacuum separation vessel and a water storage). The absorption column is used for the biogas upgrading due to water scrubbing on a random packed bed. The column is 0.3 m in diameter and around 3 m in height. An enlarged bottom column of 0.6 m diameter is used (as presented in Benizri et al. (2019) [29]) to avoid biogas leakage as the bubbles can be dragged by the liquid flow. The raw biogas is retrieved from an anaerobic digester located on the farm of Lamothe, France. Oxygen is injected in the digester to prevent hydrogen sulfide formation in the gas. The raw biogas is therefore mainly composed of carbon dioxide and methane (respectively about 40 % and 60 %) after water condensation. Activated carbon is used to ensure the absence of impurities. A gas compressor (Mauguieres MRL 100/10, France) is used to compress the gas from the digester to the column at a pressure up to 10 bars. The biogas flowrate is managed using a frequency inverter. The gas rises in the column

through the packing material and exits the column through GCV1, a back-pressure regulator that can be manually adjusted to control the pressure in the column. The water is injected at the top of the column and flows downward to the bottom of the column across the packing material where gas absorption occurs. A water level of 0.6 m measured by two pressure sensors P_1 and P_2 (Optibar P1010, Krohne, Germany) placed respectively above the interface and at the bottom of the column is maintained using a proportional electrically actuated valve (LCV1) regulated by a proportional integral derivative (PID) controller. The water flowrate Q_0 is measured with a turbine-type flowmeter from Kobold, Germany, ranging from 5 to 10 m^3/h. It is controlled by a hydraulic pump (MultiV800 from Salmson, France) frequency driven using a PID controller. The water saturated in gas exits the column by LCV1 where a pressure drop occurs (at the pressure of the GLCC). Depending on this pressure drop and the composition of the water, a certain quantity of methane and carbon dioxide degas. This multiphasic flow is separated in the GLCC. A description of the GLCC is provided in Figure 3 and a detailed description of the separation mechanisms can be found in Hreiz et al. (2014) [33,34].

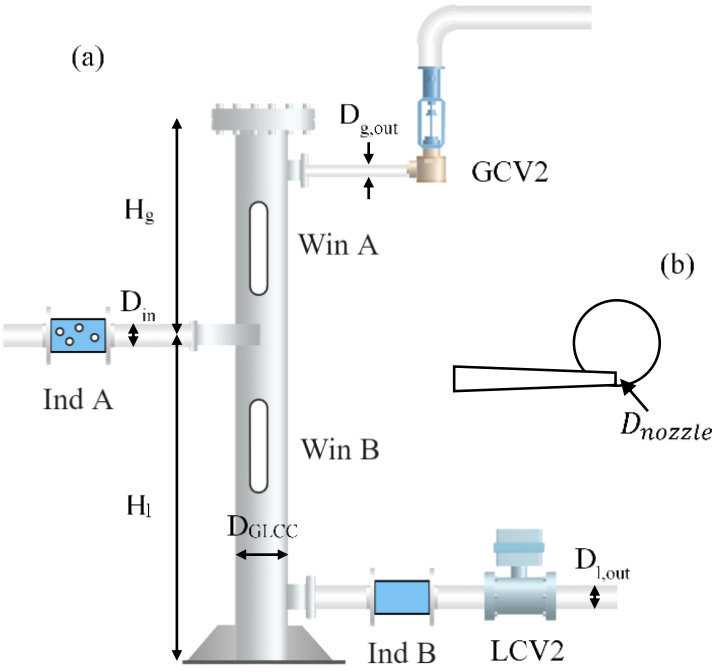

Figure 3 : Geometry and aspect design of the GLCC (a) from the side and (b) from the top.

In the GLCC, similar to the absorption column, two pressure sensors P_3 and P_4 are used to calculate the water level that is adjusted between 0.7 to 0.9 m in height with the proportionally electrically actuated valve LCV2 monitored by a PID controller. The pressure in the GLCC is set up between 2 to 6 bars in absolute pressure by controlling the gas outlet with a back-pressure regulator GCV2 that can be manually adjusted. As presented in Figure 2, the recovered gas flow can be either directly mixed with the raw biogas inlet or sent back to the digester, the latter

configuration presenting less technical issues. A by-pass section (not represented) allows to directly conduct the water to the regeneration unit without passing through the GLCC. The pipe is connected just after LCV1 and between LCV2 and the static mixer.

The water remains saturated with gas at the GLCC pressure, and therefore when exiting through the LCV2, where a second pressure drop occurs, a final degassing of the liquid is performed at the pressure of the vacuum separation vessel. This degassing is promoted by a static mixer integrated in the piping. The multiphasic flow is separated in a vessel of 1 m height and 0.6 m diameter. The gas is evacuated from the vessel by a vacuum pump (LC106 from DVP, Italy). The pressure is measured by a pressure sensor (Optibar P1010 from Krohne, Germany) and is controlled by a vacuum regulator (D51 from Emerson, USA) that can be manually adjusted from atmospheric pressure to 0.1 bar in absolute pressure. The liquid level is maintained around 0.8 m by an oscillatory level switch sensor (8111 from Bürkert, France). When the level is above the sensor, a secondary hydraulic pump is activated thanks to a frequency inverter at a frequency allowing a slight decrease in the level. When the level is below the sensor, the frequency is lowered leading to a rise in the water level. The water is sent to a water tank (2 m^3 in volume) with a cooling group for temperature control (around 288 to 293 K). The water tank is completely sealed from the atmosphere and equipped with a water bladder to withstand level variation.

The packing is initially composed of 2.65 m of RSR0.6 (plastic). A head-space allows 70 cm of additional height (3.35 m of packing in total) that were filled with two additional layers of packing: 37 cm of RSR0.3 (metal) and 33 cm of Pall Ring 0.3 (metal). Characteristics of the packings, such as the packing diameter d_p (in m), the surface area a^* (in $m^2.m^{-3}$), the void fraction ε_g (-), the number of pieces per volume N (in $pieces.m^{-3}$), and the density ρ (in $kg.m^{-3}$), are presented in Table 1.

Table 1: Characteristics of the different packing materials used in this study.

Packing Type	**d_P (m)**	**a^* (m^2/m^3)**	**ε_g**	**N (pieces.m^{-3})**	**ρ (kg.m^{-3})**
RaschigSuperRing® RSR0.6 Plastic	0.015	206	0.93	54000	62
RaschigSuperRing RSR0.3 Stainless Steel	0.0075	315	0.96	180000	230
Pall Ring 0.3	0.016	315	0.93	210000	390

Stainless Steel

2.2 Analysis material

The experimental set-up is equipped with complete sensors that allow a full description of the different stream. The biogas flowrate (Q_4) is measured using ultrasonic gas flowmeter (Optisonic 7300 Biogas from Krohne, Germany). The upgraded biomethane gas flowrate (Q_1), the recovered gas from the GLCC (Q_2) and the desorbed gas from the water regeneration unit (Q_3) are measured with a specific calibrated thermal mass flowmeter (Mass Stream D-6370 from Bronkhorst, Netherlands). The respective composition ($A_4\{y^4_{CO_2}; y^4_{CH_4}\}$, $A_1\{y^1_{CO_2}; y^1_{CH_4}\}$, $A_2\{y^2_{CO_2}; y^2_{CH_4}\}$, $A_3\{y^3_{CO_2}; y^3_{CH_4}\}$) respectively for the biogas (A_4), the bio-CH_4(A_1), the GLCC (A_2) and the bio-CO_2 (A_3) gas stream in methane and carbon dioxide are analysed using an infrared analyser X-Stream from Emerson, USA. The temperature of the gas at the inlet of the column (T1) and of the water at the outlet of the GLCC (T2) is also recorded using two PT100 sensors.

The process is monitored using an industrial computer (Programmable Logic Controller type from ARSoft Automation, France). The home-made program was developed allowing complete automated control of the device via a human-machine interface. It allows the user to set the desired parameters, and data are recorded on the computer and analyzed with a Python script to extract steady-state results. One experiment lasts about two hours, to ensure that the process is run in steady state conditions and to average the measurement for over 30 minutes to characterize the process performances.

3 Results and Discussions

The experimental campaign conducted on the farm of Lamothe (31600 Seysses, France) provided the experimental database presented in Table 2. It numbers the 36 experimental points with the parameters used (Q_0, T_2, P_1, P_3, P_5), the composition and the flowrate of the raw biogas, of the bio-CH_4, of the GLCC and of the bio-CO_2. The pressures are given in absolute pressure. The results are evaluated in terms of carbon dioxide absorption efficiency E_{CO_2} and methane recovery R_{CH_4}. Finally, characteristics concerning the configuration are given, such as the packing height implemented and whether the GLCC was directly connected to the compressor or indirectly reconnected to the digester.

Most of the previous works [25,27,35] present the absorption efficiency as an apparent diminution of the carbon dioxide purity between the biogas and the biomethane, $E^{app}_{CO_2}$ as presented in Equation (1). But it does not consider

the flow decrease and therefore the effective efficiency of the carbon dioxide absorption. A definition E_{CO_2} that considers this aspect is proposed in Equation (2), depending on the configuration of the GLCC (direct connection or indirect).

$$E_{CO_2}^{app} = \frac{y_{CO_2}^4 - y_{CO_2}^1}{y_{CO_2}^4} \quad (1)$$

$$\begin{cases} E_{CO_2} = \dfrac{y_{CO_2}^4 Q_4 + y_{CO_2}^2 Q_2 - y_{CO_2}^1 Q_1}{y_{CO_2}^4 Q_4 + y_{CO_2}^2 Q_2} \ (Direct) \\ E_{CO_2} = \dfrac{y_{CO_2}^4 Q_4 - y_{CO_2}^1 Q_1}{y_{CO_2}^4 Q_4} \ (Indirect) \end{cases} \quad (2)$$

The methane recovery ratio R_{CH_4} is also calculated. It represents the methane recovered from the device compared to the inlet, and therefore the methane losses. Two expressions can be given for R_{CH_4}, respectively considering only the methane that is recovered from the biomethane outlet compared to the gas entering the column ($R_{CH_4}^{col}$), and considering the overall methane that is not lost through the bioCO_2 outlet ($R_{CH_4}^{glob}$). Depending on the GLCC outlet configuration, two expressions can be proposed for each configuration, as presented in Equation (3) and (4).

$$\begin{cases} R_{CH_4}^{col} = \dfrac{y_{CH_4}^1 Q_1}{y_{CH_4}^4 Q_4 + y_{CH_4}^2 Q_2} \ (Direct) \\ R_{CH_4}^{col} = \dfrac{y_{CH_4}^1 Q_1}{y_{CH_4}^4 Q_4} \ (Indirect) \end{cases} \quad (3)$$

$$\begin{cases} R_{CH_4}^{glob} = \dfrac{y_{CH_4}^1 Q_1}{y_{CH_4}^4 Q_4} \ (Direct) \\ R_{CH_4}^{glob} = \dfrac{y_{CH_4}^1 Q_1 + y_{CH_4}^2 Q_2}{y_{CH_4}^4 Q_4} \ (Indirect) \end{cases} \quad (4)$$

The database presented in Table 2 does not show results at 40 Nm^3/h, which is due to experimental limitations. The on-site configuration imposes a certain distance between the container and the digester, and the gas was deviated from the main line downstream of a condensate vessel. The gas has to be sucked from the digester over the entire piping line ending in a vacuum in the piping system. This vacuum causes a decrease in the compressor flowrate that was consequently not capable of reaching the 40 Nm^3/h. Also, the gas analysis shows that a slight variation occurs in the gas composition, with the respective composition of carbon dioxide and methane that does not reach 100 %. Gas analysis were conducted using gas chromatography (results not shown) to identify the compounds. The remaining gas was air, that was attributed to a slight aspiration in the piping device. For the

purpose of comparison between experiments, the gas fraction was normalized ($\bar{y}^1_{CH_4}$) regarding only the fraction of methane and carbon dioxide as presented in Equation (5).

$$\bar{y}^i_{CH_4} = \frac{y^i_{CH_4}}{y^i_{CH_4} + y^i_{CO_2}} \quad (5)$$

In addition, the bio-CO_2 gas outlet was highly humid especially at low pressures, leading to technical issues. The vacuum pump was equipped with an exhaust mist eliminator that injects air in the gas flow while pumping. It allows to reduce the mist from the gas flow, but a fraction of air is present in the gas, leading to air in bio-CO_2 outlet. This gas outlet was also normalized ($\bar{y}^3_{CH_4}$) according to Equation (5) and the gas flowrate was calculated as $Q_3 = Q_4 - Q_1 - Q_2$.

Table 2: Experimental database obtained from the measurement campaign at the farm of Lamothe (France).

	Parameters					Biogas			Bio-CH_4				GLCC			Bio-CO_2				Results			Configuration	
N	Q_0 m^3/h	T_2 K	P_1 bar	P_3 bar	P_5 bar	$y^4_{CO_2}$	$y^4_{CH_4}$	Q_4 Nm^3/h	$y^1_{CO_2}$	$y^1_{CH_4}$	$\bar{y}^1_{CH_4}$	Q_1 Nm^3/h	$y^2_{CO_2}$	$y^2_{CH_4}$	Q_2 Nm^3/h	$y^3_{CO_2}$	$y^3_{CH_4}$	$\bar{y}^3_{CH_4}$	Q_3 Nm^3/h	E_{CO_2}	$R^{glob}_{CH_4}$	$R^{col}_{CH_4}$	H_{col}	GLCC
1	5.0	303	6.8	0.0	0.79	0.38	0.60	18.9	0.20	0.74	0.79	11.5	0.00	0.00	0.0	0.79	0.13	0.14	7.4	0.66	0.80	0.80	2.65	Direct
2	5.0	301	7.1	0.0	0.50	0.37	0.58	19.7	0.13	0.82	0.86	12.1	0.00	0.00	0.0	0.81	0.12	0.13	7.6	0.77	0.92	0.92	2.65	Direct
3	5.0	299	7.0	0.0	0.32	0.37	0.60	18.5	0.10	0.84	0.89	12.4	0.00	0.00	0.0	0.77	0.16	0.17	6.1	0.80	0.99	0.99	2.65	Direct
4	5.0	301	7.1	3.2	0.81	0.37	0.60	19.2	0.19	0.75	0.80	13.8	0.48	0.51	3.3	0.79	0.14	0.15	5.4	0.68	0.96	0.84	2.65	Direct
5	5.0	299	6.9	2.2	0.82	0.36	0.56	19.1	0.24	0.75	0.76	13.6	0.68	0.31	11.2	0.86	0.06	0.06	5.5	0.77	0.97	0.73	2.65	Direct
6	5.0	299	7.1	5.5	0.82	0.35	0.59	20.5	0.19	0.79	0.80	13.7	0.32	0.68	1.0	0.78	0.15	0.16	6.8	0.64	0.91	0.86	2.65	Direct
7	7.0	299	8.7	4.2	0.42	0.37	0.61	19.3	0.11	0.86	0.89	12.0	0.33	0.68	11.9	0.77	0.16	0.17	7.3	0.88	0.91	0.54	2.65	Direct
8	5.0	300	7.0	5.1	0.81	0.37	0.60	19.8	0.22	0.76	0.78	13.0	0.38	0.63	1.3	0.84	0.14	0.14	6.8	0.63	0.85	0.80	2.65	Direct
9	6.0	307	8.8	0.0	0.34	0.37	0.58	19.6	0.06	0.85	0.94	11.3	0.00	0.00	0.0	0.78	0.18	0.18	8.3	0.90	0.93	0.93	2.65	Direct
10	5.0	309	8.9	5.5	0.28	0.36	0.61	19.4	0.06	0.87	0.94	12.0	0.36	0.61	1.2	0.82	0.11	0.12	7.4	0.90	0.95	0.89	2.65	Direct
11	5.0	306	9.1	4.5	0.82	0.37	0.61	17.9	0.14	0.82	0.86	11.7	0.48	0.54	6.7	0.81	0.10	0.11	6.2	0.83	0.92	0.69	2.65	Direct
12	9.0	307	9.0	4.8	0.82	0.39	0.61	18.3	0.14	0.85	0.86	10.6	0.33	0.70	3.5	0.71	0.19	0.21	7.7	0.82	0.82	0.67	2.65	Direct
13	6.0	302	9.0	0.0	0.35	0.39	0.59	21.1	0.12	0.86	0.87	12.3	0.00	0.00	0.0	0.74	0.18	0.20	8.8	0.81	0.87	0.87	2.65	Direct
14	2.9	303	8.9	0.0	0.33	0.39	0.59	21.0	0.15	0.82	0.85	12.8	0.00	0.00	0.0	0.81	0.10	0.11	8.2	0.76	0.87	0.87	2.65	Indirect
15	5.0	290	6.8	0.0	0.50	0.40	0.62	20.4	0.17	0.82	0.83	12.9	0.00	0.00	0.0	0.74	0.16	0.18	7.5	0.73	0.85	0.85	2.65	Indirect
16	5.0	292	6.8	2.2	0.49	0.40	0.61	20.4	0.18	0.82	0.82	12.8	0.35	0.65	2.8	0.80	0.09	0.10	4.8	0.72	0.99	0.84	2.65	Indirect
17	8.0	291	8.8	2.5	0.51	0.40	0.61	20.4	0.09	0.90	0.91	9.9	0.34	0.65	4.7	0.74	0.15	0.16	5.8	0.89	0.97	0.72	2.65	Indirect
18	6.0	287	9.0	2.4	0.29	0.40	0.60	20.4	0.10	0.89	0.90	10.9	0.44	0.58	4.1	0.78	0.13	0.14	5.5	0.87	0.99	0.80	2.65	Indirect
19	8.0	288	9.1	2.6	0.27	0.39	0.60	20.4	0.05	0.91	0.95	10.1	0.33	0.66	4.6	0.75	0.17	0.18	5.8	0.93	1.02	0.78	2.65	Indirect
20	9.0	290	8.9	2.9	0.60	0.38	0.59	20.5	0.09	0.86	0.91	9.9	0.37	0.60	4.7	0.71	0.17	0.20	6.0	0.88	0.98	0.75	2.65	Indirect
21	5.0	288	9.0	4.2	0.23	0.37	0.59	19.4	0.09	0.86	0.91	11.7	0.25	0.72	6.1	0.75	0.15	0.17	1.5	0.85	1.32	0.93	2.65	Indirect
22	8.0	288	9.0	4.9	0.49	0.38	0.63	31.5	0.11	0.89	0.89	17.3	0.29	0.71	2.9	0.75	0.19	0.20	11.3	0.84	0.88	0.78	2.65	Indirect

	Parameters					Biogas			Bio-CH4				GLCC			Bio-CO2				Results			Configuration	
N	Q_0 m^3/h	T_2 K	P_1 bar	P_3 bar	P_5 bar	$y^4_{CO_2}$	$y^4_{CH_4}$	Q_4 Nm^3/h	$y^1_{CO_2}$	$y^1_{CH_4}$	$\bar{y}^1_{CH_4}$	Q_1 Nm^3/h	$y^2_{CO_2}$	$y^2_{CH_4}$	Q_2 Nm^3/h	$y^3_{CO_2}$	$y^3_{CH_4}$	$\bar{y}^3_{CH_4}$	Q_3 Nm^3/h	E_{CO_2}	$R^{glob}_{CH_4}$	$R^{col}_{CH_4}$	H_{col} m	GLCC
23	6.0	289	9.3	4.0	0.30	0.38	0.61	20.4	0.07	0.92	0.93	12.1	0.35	0.65	2.7	0.73	0.20	0.22	5.6	0.89	1.05	0.91	2.65	Indirect
24	8.0	289	9.5	3.5	0.29	0.38	0.61	28.9	0.08	0.90	0.92	14.8	0.33	0.65	3.7	0.78	0.16	0.17	10.4	0.89	0.91	0.77	2.65	Indirect
25	8.0	289	8.9	3.5	0.82	0.38	0.61	28.4	0.13	0.85	0.86	16.2	0.44	0.56	3.4	0.73	0.17	0.19	8.8	0.80	0.92	0.81	2.65	Indirect
26	8.0	290	7.0	3.1	0.52	0.38	0.61	29.7	0.14	0.84	0.86	17.0	0.42	0.57	1.3	0.77	0.14	0.15	11.4	0.78	0.85	0.81	2.65	Indirect
27	6.0	289	8.9	3.2	0.29	0.38	0.61	29.1	0.12	0.85	0.88	17.1	0.40	0.59	9.9	0.80	0.12	0.13	2.1	0.81	1.17	0.85	2.65	Indirect
28	6.0	289	9.6	3.4	0.26	0.38	0.62	20.3	0.04	0.95	0.96	10.2	0.34	0.66	7.0	0.79	0.12	0.13	3.1	0.95	1.15	0.78	3.35	Indirect
29	6.0	290	10.0	3.4	0.28	0.39	0.61	20.0	0.04	0.94	0.96	10.5	0.33	0.67	3.9	0.78	0.14	0.15	5.6	0.95	1.04	0.83	3.35	Indirect
30	8.0	291	9.7	3.5	0.27	0.39	0.60	19.9	0.04	0.94	0.96	9.6	0.28	0.71	4.3	0.74	0.18	0.20	6.0	0.95	1.02	0.77	3.35	Indirect
31	7.9	292	9.7	3.7	0.33	0.39	0.60	29.9	0.05	0.92	0.95	15.4	0.31	0.67	4.3	0.81	0.13	0.13	10.2	0.93	0.98	0.82	3.35	Indirect
32	6.0	292	9.6	1.6	0.21	0.39	0.61	19.9	0.03	0.94	0.97	9.2	0.49	0.50	5.3	0.81	0.08	0.09	5.4	0.96	0.95	0.73	3.35	Indirect
33	6.0	287	9.5	3.3	0.23	0.39	0.61	20.5	0.03	0.95	0.97	9.4	0.31	0.67	1.9	0.80	0.11	0.12	9.2	0.96	0.83	0.73	3.35	Indirect
34	6.0	292	9.9	3.5	0.30	0.38	0.60	20.6	0.06	0.91	0.94	11.5	0.33	0.65	5.0	0.79	0.13	0.14	4.1	0.91	1.14	0.87	3.35	Indirect
35	6.0	290	10.0	1.6	0.20	0.39	0.61	19.4	0.03	0.95	0.97	8.9	0.48	0.51	5.5	0.80	0.09	0.10	5.0	0.97	0.96	0.73	3.35	Indirect
36	6.0	289	10.0	1.8	0.24	0.38	0.60	33.5	0.04	0.93	0.95	16.8	0.63	0.34	6.8	0.86	0.05	0.06	9.9	0.94	0.91	0.80	3.35	Indirect

3.1 Process operation and repeatability

Process operation is of major importance to evaluate the process efficiency and its reliability. Malfunctions were identified on several industrial processes leading for example to methane losses. It can also endanger the safety of the installation and the reliability of the production [22,27,36]. A typical dynamic of an experiment is given in Figure 4 presenting the main regulated parameters and the results of the process. The example given is from experiment number 30.

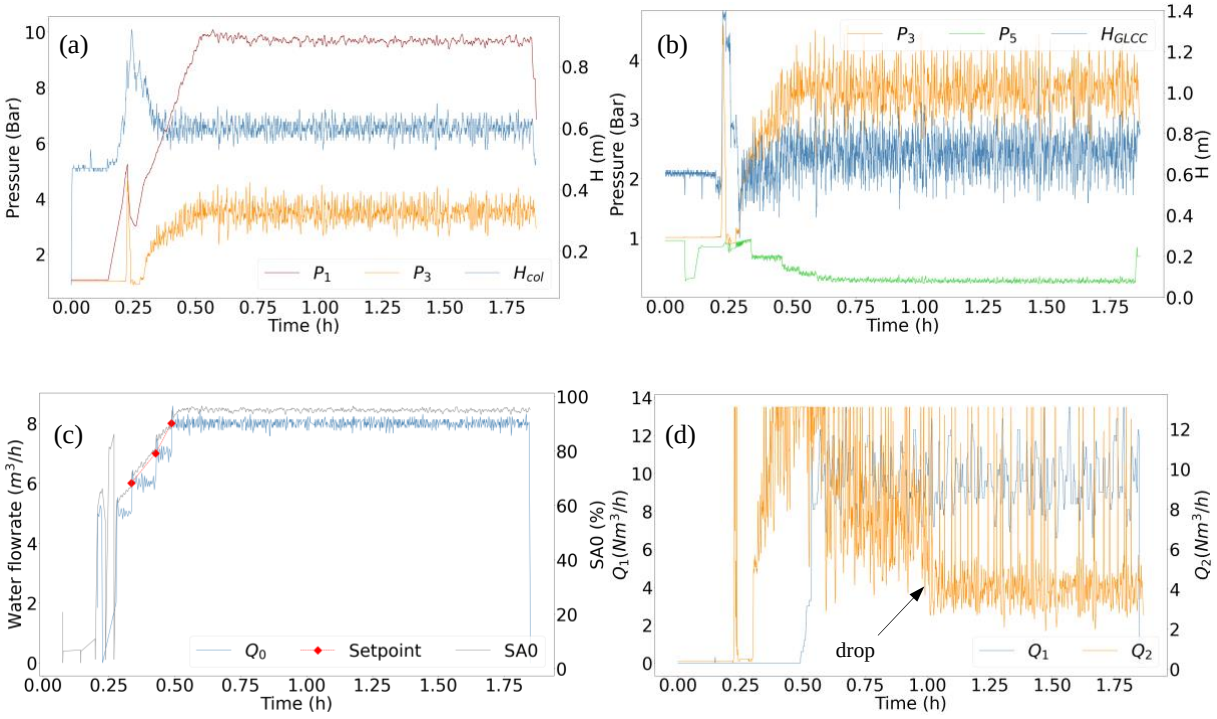

Figure 4: Typical dynamic of the process during a complete experiment (N°.30) with the regulation of (a) the column, (b) the GLCC, (c) the water pumping and (d) the gas flowrates.

Figure 4 (a) and (b) show respectively the water level and the pressure outstream and downstream from the regulation valve of (a) the column and (b) the GLCC. The process seems to be stabilized after 1 hour (about 0.5 hour after the nominal water flowrate is reached). The water flowrate, as illustrated in (c), is incremented up to the final desired setpoint and the response is almost immediate and remains stable during the experiment. The pressures P_1, P_3, and P_5 oscillate around the setpoints with no deviation in time once settled, just as the water levels in the column and in the GLCC, ensuring no gas leaks. The water level in the GLCC oscillates in a range of ± 20 cm around the setpoint, and is associated to pressure oscillation and therefore gas flowrate oscillation as presented in (d). These oscillations are due to the small residence time (around 5 s) that complicates the regulation of the level. Nevertheless, it allows sufficient regulation of the level with no disruption. Finally, the gas flowrate in the GLCC (Q_2) drops around 1 hour (about 0.5 hour after the stabilization of the other parameters), meaning

that in this case, the steady state of the experiment is obtained one hour after the experiment started. This delay might be due to the time required by the whole set up to recirculate the water so that each part is in a steady-state. A complete circulation of the water in the device at 8 m^3/h is obtained in around 30 minutes. The experimental results presented in Table 2 are the average values (usually from a 0.5-hour duration) obtained once the steady-state is reached.

Another point that is crucial for the process evaluation is the repeatability of an experiment. The experiments number 15 and 16 present almost the same parameters: Q_0 at 5 m^3/h , T_2 at 290 K, P_1 at 7 bars, P_5 at 0.5 bar, the biogas composition was 0.4 and 0.6 in carbon dioxide and in methane respectively, and Q_4 was around 20 Nm^3/h. The column height was 2.65 m and the GLCC was indirectly connected. The only difference is for the GLCC: In experiment 15, it was by-passed and in experiment 16, a pressure of 2.2 bars was applied. Also, experiments 32, 33 and 35 are close enough to be compared. Q_0 is at 6 m^3/h , T_2 at 290 K, P_1 at 9.7 bars, P_5 at 0.22 bar, the biogas composition was 0.38 and 0.6 in carbon dioxide and in methane respectively, and Q_4 was around 20 Nm^3/h. The column height was 3.35 m, and the GLCC was indirectly connected. Again, the only difference is for the GLCC: In experiment 32 and 35, a pressure of 1.6 bars was applied and in experiment 33 a pressure of 3.3. The results are presented in Figure 5.

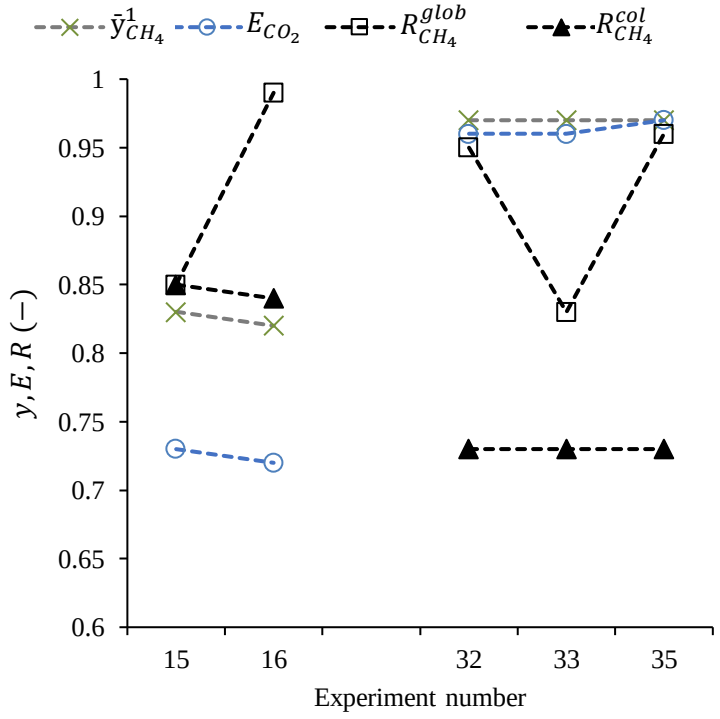

Figure 5: Evaluation of the repeatability on the upgrading performances ($\bar{y}^1_{CH_4}$, E_{CO_2}, $R^{glob}_{CH_4}$ and $R^{col}_{CH_4}$) for two experiments in similar operating conditions.

The three parameters $\bar{y}_{CH_4}^1$, E_{CO_2} and $R_{CH_4}^{col}$ present almost the same values. $R_{CH_4}^{glob}$ highly increases in experiment 16 compared to experiment 15, due to the GLCC configuration that returns the methane to the digester. In experiment 33, $R_{CH_4}^{glob}$ decreases compared to experiment 32 and 35 because as the pressure in the GLCC is higher, less methane is recovered. Yet in both cases, the GLCC configuration in both cases does not affect any other parameter. While this comparison confirms the repeatability of an experiment when the same parameters are used, more comparisons should be conducted to corroborate this repeatability and also to evaluate the sensitivity of the results regarding parameters variations.

3.2 Effect of absorption pressure, water temperature and water flowrate on the performances

Water temperature (T_2), water flowrate (Q_0), and absorption pressure in the column (P_1) are common parameters that were identified in the literature to influence the process performances. Their influences for this scrubbing configuration are discussed in the following part.

Concerning the water temperature, two sets of experiments were used to describe the influence on the process: experiments number 2 (301 K) and 15 (290 K) and experiments number 10 (309 K) and 21 (288 K), described in Table 3.

Table 3: Average values of the parameters of the two sets of experiments used to characterize the influence of the temperature.

Set (Experiment number)	Q_0 **(m³/h)**	P_1 **(bar)**	P_3 **(bar)**	T_2 **(K)**	Q_4 **(Nm³/h)**	P_5 **(bar)**
1(2,15)	5.0	7.0	/	290 – 301	19.7	0.5
2(10,21)	5.0	9.0	5	288 – 309	19.4	0.25

The results are presented in Figure 6. It shows a slight decrease in y_{CH_4}, E_{CO_2} and R_{CH_4}, except for the second set where $R_{CH_4}^{glob}$ highly increases over 1. This value could be attributed to the different configuration of the GLCC and probably a misevaluation of its flowrate Q_2. As illustrated in Figure 4, the drop in the GLCC flowrate might have not been reached, leading to overestimation of the recirculated methane. Nevertheless, this result is still quite surprising, as with the decrease in temperature, absorption should be enhanced according to Henry's law. This influence is well described in the literature concerning common HPWS with an experimental or modelling approach [24,37,38]. But as the water is in closed-loop, the regeneration also depends on the temperature, and in contrast to the absorption, a decrease in temperature lowers the regeneration efficiency. This experimental assessment confirms the assumption proposed by Wantz et al. (2022) through a modelling description [30].

Therefore, it seems inefficient to aim for water refrigeration that requires a great amount of energy whereas the benefit is compensated by a poor desorption efficiency.

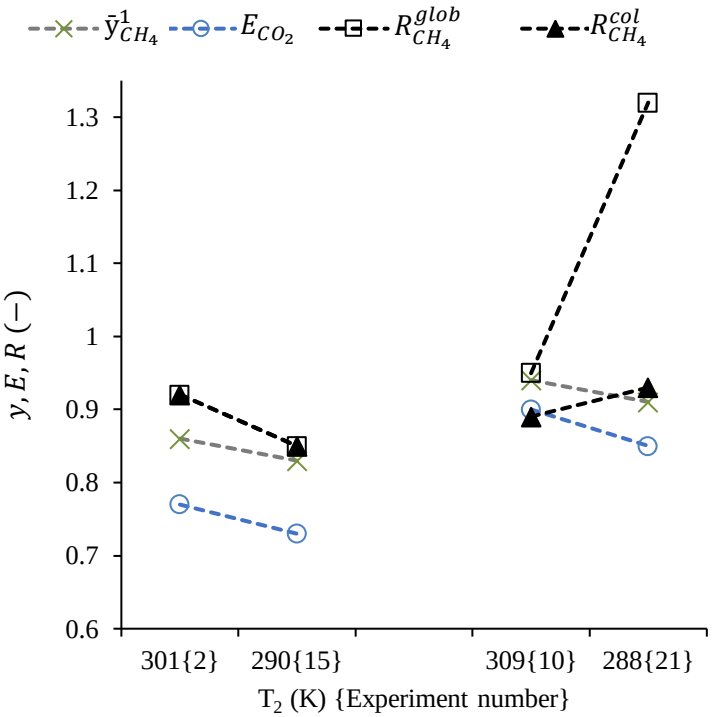

Figure 6: Effect of the water temperature on the upgrading performances ($\tilde{y}^1_{CH_4}$, E_{CO_2}, $R^{glob}_{CH_4}$ and $R^{col}_{CH_4}$).

The water flowrate influence is also investigated in this work using five sets of experiments. The average values are given in Table 4 and the results are presented in Figure 7.

Table 4: Average values of the parameters of the five sets of experiments used to characterize the influence of the water flowrate.

Set (Experiment number)	$\boldsymbol{Q_0}$ **(m^3/h)**	$\boldsymbol{P_1}$ **(bar)**	$\boldsymbol{P_3}$ **(bar)**	$\boldsymbol{T_2}$ **(K)**	$\boldsymbol{Q_4}$ **(Nm^3/h)**	$\boldsymbol{P_5}$ **(bar)**
1(11,12)	5 - 9	9	4.7	307	18	0.8
2(18,19)	6 - 8	9	2.5	290	20	0.3
3(29,30)	6 - 8	10	3.5	290	20	0.3
4(14,13)	3 - 6	9	0	300	21	0.3
5(27,24)	6 - 8	9	3.5	290	30	0.3

The influence of the water flowrate on the process performances is more complicated to evaluate. At first glance, $\tilde{y}^1_{CH_4}$ and E_{CO_2} globally increase (or stagnate) when $R^{col}_{CH_4}$ and $R^{glob}_{CH_4}$ decrease while the flowrate decreases. When looking more closely at the detailed parameters, some trend can be identified. Indeed, the regeneration for Set

number 1 is conducted at 0.8 bar, which is associated to a poor desorption (see section 3.3). Therefore, little amounts of gas can be absorbed in the liquid when circulating through the column. When increasing the water flowrate, it appears that only methane absorption increases lowering R_{CH_4}. Under these conditions, rising the water flowrate lowers the performances of the process and is also associated to a higher energy consumption. Set 2 presents similar parameters but the desorption is conducted at 0.3 bar. With this condition, the regeneration is enhanced and the water shows higher absorption capacity. Consequently, increasing the water flowrate from 6 to 8 m^3/h is associated to higher methane purity and absorption efficiency as illustrated in Figure 7. Set 4 is in similar conditions but with a lower flowrate, from 3 to 6 m^3/h and it is also associated to an increase in methane purity and absorption efficiency. This corroborates that a proper water flowrate has to be implemented for optimal absorption efficiency. Set 3 is performed with similar parameters as Set 2, but with an increase in the packing height. This time, 6 m^3/h seems to be sufficient for absorption as at 8 m^3/h, no gain on methane purity and absorption efficiency is obtained. This illustrates the entanglement between the mass transfer occurring in the column and the resulting performances. Finally, Set 5 is in similar conditions but with a higher biogas flowrate (around 30 Nm^3/h) and this time, increasing the water flowrate from 6 to 8 m^3/h leads to an increase in the absorption efficiency and methane purity. Water flowrate increase is commonly associated to higher E_{CO_2} and lower $R_{CH_4}^{col}$ but it does not consider the influence of the regeneration [24,25]. It is probably the case for lower water flowrates as presented in Benizri et al. (2019) [29], but once a certain maximal value is reached, E_{CO_2} stagnates and $R_{CH_4}^{col}$ decreases. One can conclude that for given operating conditions, if desorption is sufficient and the packing height is enough, the water flowrate can be the adjustable variable regarding the biogas flowrate. This should facilitate the operating of the device by adjusting only one parameter.

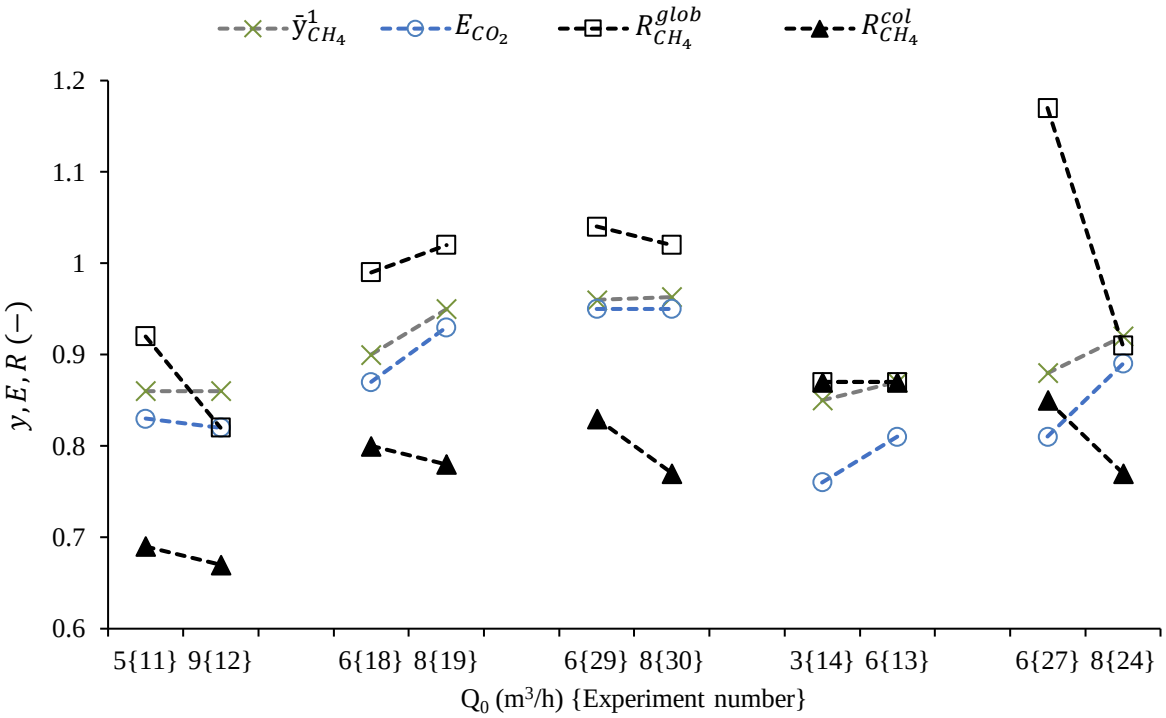

Figure 7: Water flowrate influence on the upgrading performances ($\tilde{y}^1_{CH_4}$, E_{CO_2}, $R^{glob}_{CH_4}$ and $R^{col}_{CH_4}$).

Finally, the influence of the absorption pressure P_1 is evaluated. Experiments 8 and 11 were compared, with an increase in the pressure from 7 to 9, so experiments number 26 and 22, and described in Table 5. The results are presented in Figure 8.

Table 5: Average values of the parameters of the two sets of experiments used to characterize the influence of the absorption pressure.

Set (Experiment number)	Q_0 (m³/h)	P_1 (bar)	P_3 (bar)	T_2 (K)	Q_4 (Nm³/h)	P_5 (bar)
1(8,11)	5.0	7.0 – 9.0	4.8	303	18.9	0.8
2(26,22)	8.0	7.0 – 9.0	4.0	290	30.5	0.5

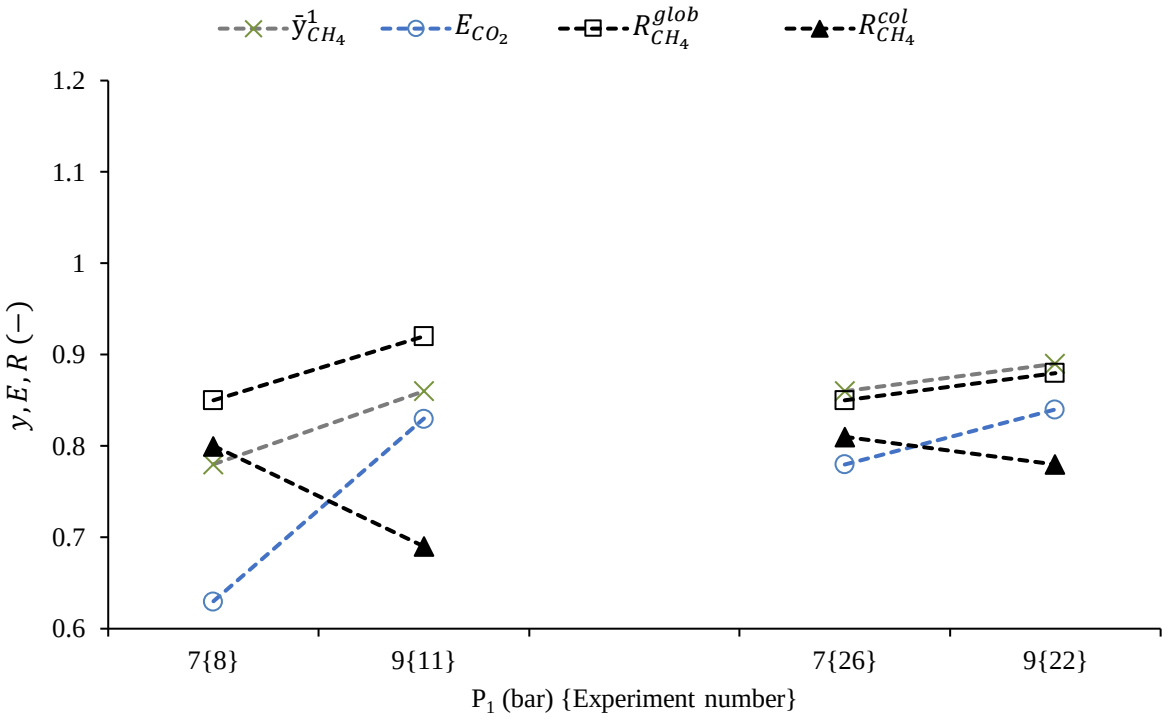

Figure 8: Effect of absorption pressure P_1 on the process performances ($\bar{y}^1_{CH_4}$, E_{CO_2}, $R^{glob}_{CH_4}$ and $R^{col}_{CH_4}$).

In each case, an increase of P_1 is associated to an increase in $\bar{y}^1_{CH_4}$ and in E_{CO_2}. High methane purity could be obtained by increasing the pressure, but it is also associated to higher methane losses in the column, as $R^{col}_{CH_4}$ decreases. This negative effect can be attenuated using the GLCC, especially for experiment 8 and 11, and 26 and 22, as it allows to increase $R^{glob}_{CH_4}$. So $P_1$is a parameter that should be set with great attention to prevent excessive energy consumption and methane leaks, but it is necessary to implement sufficient pressure to reach the desired methane purity. Associated methane leaks can be reduced by using the GLCC.

3.3 Influence of the vacuum desorption pressure on the performances

The vacuum applied on the water flow that aims to enhance the desorption of the gases is one of the most innovative contributions of this work, as no experimental assessment of this influence is proposed in the literature for biogas. upgrading. The database established during the experimental campaign allows to evaluate the influence of this pressure on four sets of experiments, with the average values of the parameters presented in Table 6. The results are presented in Figure 9. The experimental results were also compared to the simulated values obtained thanks to the theoretical model developed by Wantz et al. (2022) [30].

Table 6: Average values of the parameters of the four sets of experiments used to characterize the influence of the vacuum pressure.

Set (Experiment number)	Q_0 **(m^3/h)**	P_1 **(bar)**	P_3 **(bar)**	T_2 **(K)**	Q_4 **(Nm^3/h)**	P_5 **(bar)**
1(1,2,3)	5	7	0	300	20	0.8,0.5,0.3
2(11,10)	5	9	5	308	19	0.8,0.3
3(17,19)	8	9	2.5	290	20	0.5,0.3
4(25,22)	8	9	4	290	30	0.8,0.5

The results show a significant improvement of the biomethane purity associated to a higher carbon dioxide elimination rate. The recovery of methane is also improved, except for the set number 4 that might be due to a gap in the pressure P_3 (3.5 and 4.9 respectively for experiment number 25 and 22). The Set number 1 was especially conducted to assess the impact of P_5 on the process. The GLCC was not used to avoid any concomitant effect and three different pressures of 0.8, 0.5 and 0.3 bar were applied to highlight a clear trend. This set shows a great improvement of the methane purity and the carbon dioxide elimination rate with the diminution of the pressure. These results agree with Henry's law, and it can be concluded that the rough vacuum applied promote the gas desorption and the regeneration of the water, which in turn shows higher capacities for absorption. It also illustrates that the gain is higher when reducing the pressure from 0.8 to 0.5 than from 0.5 to 0.3. This phenomenon was already discussed in Wantz et al. (2022) [30] using a modeling approach, and this experimental corroboration emphasizes both the interest of applying a rough vacuum on the regeneration but also to limit its lower value. Indeed, applying an excessive vacuum would be associated to unnecessary power requirements with no gain on the process performances.

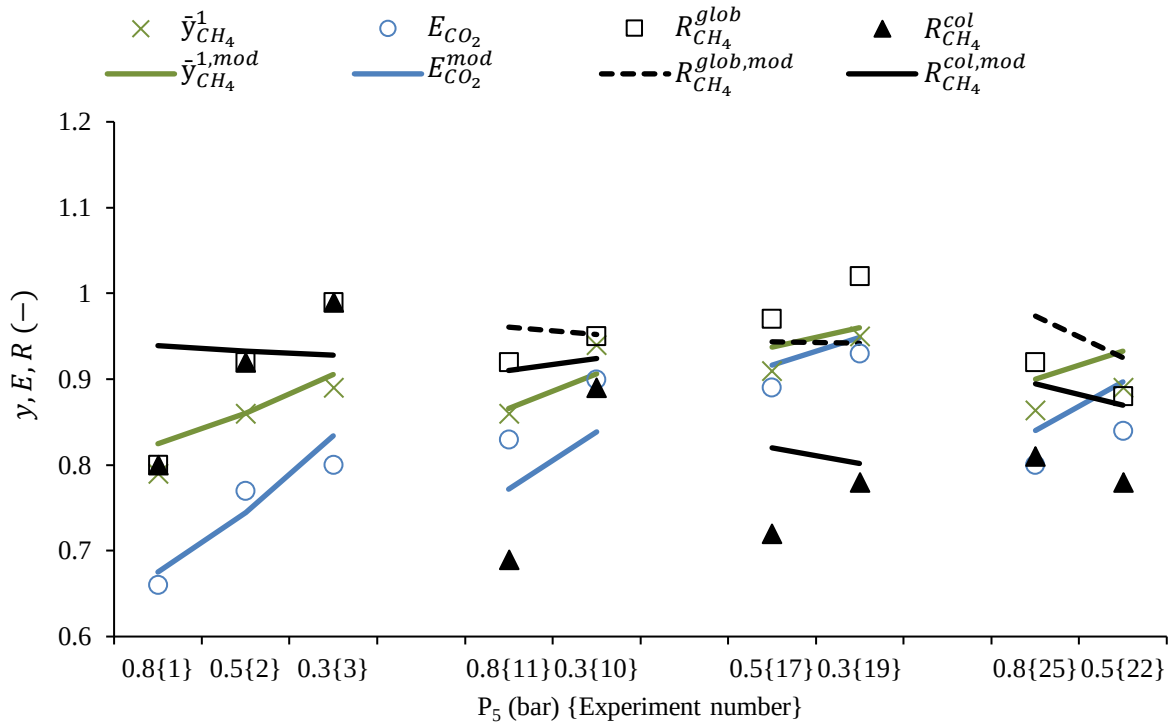

Figure 9: Effect of the vacuum regeneration pressure P_5 on the upgrading performances ($\bar{y}^{1}_{CH_4}$, E_{CO_2}, $R^{glob}_{CH_4}$ and $R^{col}_{CH_4}$) and comparison with the model of Wantz et al. (2022) [30].

3.4 Influence of the packing height and optimization of the mass transfer

The packing height of the column was increased to assess the influence on the process efficiency. The column height offered the possibility to add 70 cm of packing on top of the 2.65 m of RSR 0.6 (plastic), that were filled with two additional layers of packing: 37 cm of RSR 0.3 (stainless steel) and 33 of Pall rings (stainless steel). Experiment number 23 and 28 present similar conditions at a biogas flowrate around 20 Nm^3/h, and experiment number 24 and 31 at around 30 Nm^3/h. The results are illustrated in Figure 10.

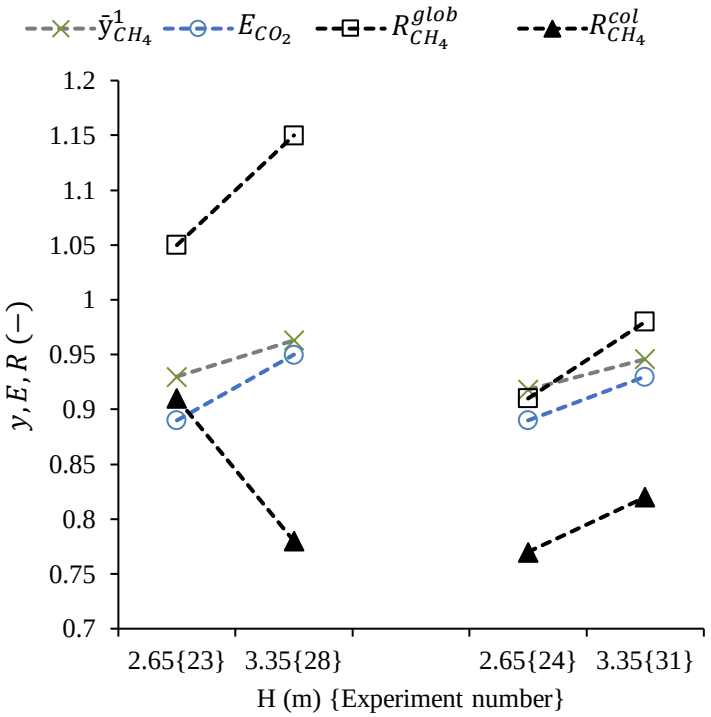

Figure 10: Effect of the packing height on the upgrading performances ($\bar{y}^1_{CH_4}$, E_{CO_2}, $R^{glob}_{CH_4}$ and $R^{col}_{CH_4}$).

The results obtained for these configurations show the determining influence of the packing height on the performance of the absorption. Regardless of the biogas flowrate, the packing height allows to improve E_{CO_2}, R_{CH_4} and y_{CH_4} significantly. At 20 Nm^3/h, these parameters are respectively raised from 0.90, 1.05 and 0.93 to 0.96, 1.15 and 0.96. At 30 Nm^3/h, from 0.9, 0.91 and 0.92 to 0.98, 0.94 and 0.95. Such results were expected as more time and interfacial area are available for absorption. But the water regeneration is still relevant at this high absorption rate. Moreover, this slight increase in the packing height allows to reach over 97 % of methane purity in the biomethane, for example in experiment number 35, unravelling the possibility for gas grid injection.

The raise of column height necessarily comes along with an increase of manufacturing costs. However, as discussed in the following, possibilities remain to shorten the column height while maintaining the performances. Indeed, to the authors' knowledge, no research was addressed to characterize the hydrodynamics in the column for biogas absorption. HPWS for biogas upgrading is a very specific application of packing columns. Indeed, the liquid to gas ratio is particularly high, the column is under pressure, and the gas flow decreases from around 50 % between the inlet and the outlet of the column, strongly modifying the hydrodynamic behavior along the packing.

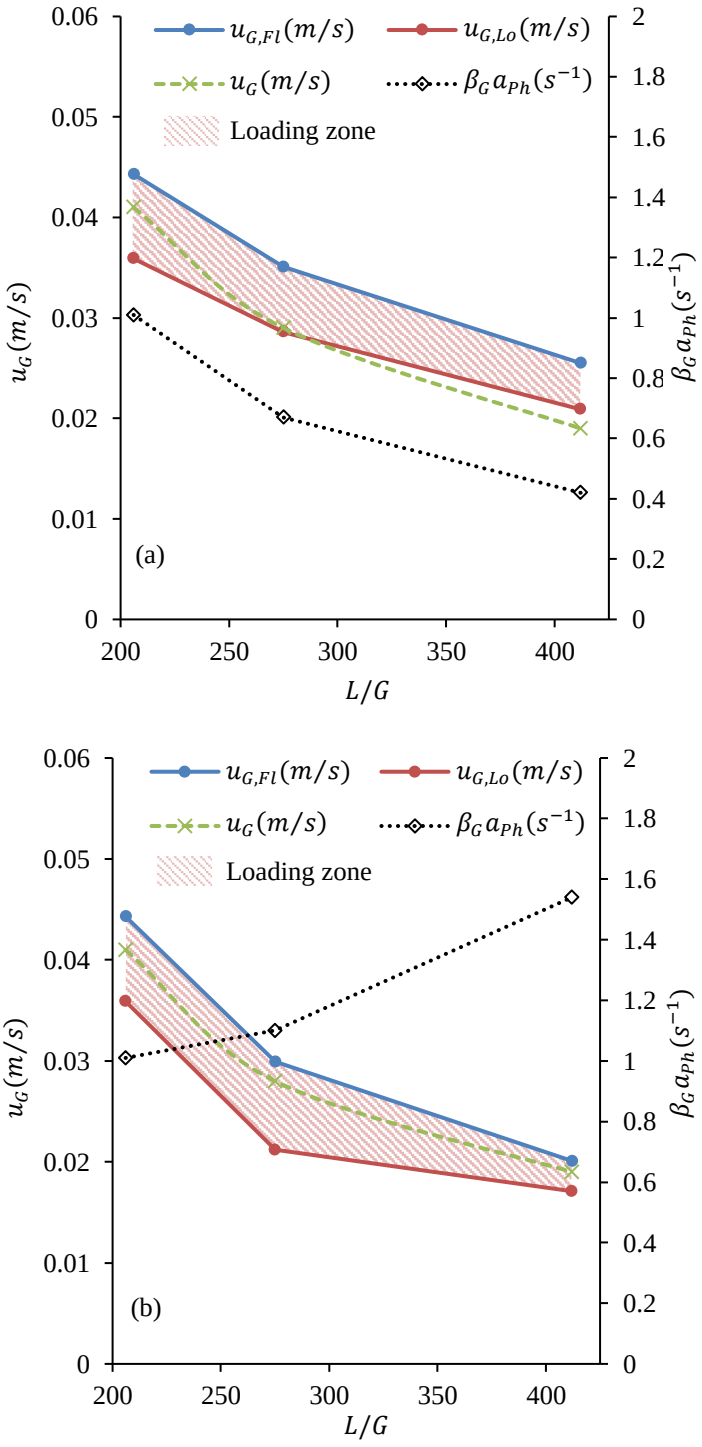

Figure 11: Flooding, loading, effective gas velocities (respectively $u_{G,Fl}$, $u_{G,Lo}$, and u_G in m/s), and volumetric mass transfer coefficients ($\beta_G a_{Ph}$ in s^{-1}) with the increase of the liquid to gas ratio (L/G from 206, 275 and 412) due to gas absorption corresponding to a gas flowrate decrease from 40, 30 to 20 Nm^3/h, a liquid flowrate of 10 m^3/h, a pressure of 10 bars and a 0.2 m column diameter using (a) RSR 1 packing and (b) an evolutive packing (RSR 1, Hiflow 25 and RSR 0.5), calculated from Billet-Schultes correlations [39].

Billet-Schultes correlations [39] were used to evaluate the loading and flooding gas velocities ($u_{G,Lo}$ and $u_{G,Fl}$ in $m.s^{-1}$) and the volumetric mass transfer coefficient ($\beta_G a_{Ph}$ in s^{-1}) of this column configuration. Parameters used in the beginning were 20 Nm^3/h of biogas flowrate, water flowrate of 6 m^3/h and P_1 at 10 bars. Then, calculations were conducted at 40 Nm^3/h of biogas flowrate, with a water flowrate of 10 m^3/h, and P_1 at 10 bars. RSR1 (metal) was taken as a packing as the one used (RSR0.6 plastic) is not characterize in the literature but presents the most similar characteristics. At 20 Nm^3/h, the correlations give a flooding velocity of 0.016 m/s, a loading velocity of 0.0098 m/s, and the actual gas velocity is of 0.0084 m/s and at 40 Nm^3/h, the correlations give a flooding velocity of 0.035 m/s, a loading velocity of 0.029 m/s, and the actual gas velocity is of 0.017 m/s. This result highlights that the column is working far beyond the loading point and a gain in mass transfer could be obtained by reducing the column diameter.

Billet-Schultes correlations were then applied to evaluate the loading and flooding conditions for a biogas flowrate of 40 Nm^3/h, a packed column reduced to 0.2 m diameter filled with RSR 1 (metal), at a water flowrate of 10 m^3/h under 10 bars. The liquid to gas ratio increases with the column height considering that the biogas flowrate at the top of the column reaches 20 Nm^3/h. The initial biogas flowrate of 40 Nm^3/h, an intermediate flowrate of 30 Nm^3/h, and the final gas flowrate of 20 Nm^3/h correspond to respective liquid to gas ratios of 206, 275 and 412. Results are presented in Figure 11 (a). It shows that for the selected conditions, it is expected that the column works within the loading zone at the bottom of the packing, giving the best conditions for mass transfer (around 1 s^{-1} for the volumetric mass transfer coefficient $\beta_G a_{Ph}$ in this case). But with the decrease in the gas flowrate due to absorption, the gas velocity rapidly decreases, and the working conditions deviate from the expected behavior, associated to a drop in the mass transfer coefficients and therefore lower absorption performances, as illustrated in Figure 11 (a).

Simulation were performed again but with an evolution in the packing characteristics to evaluate the feasibility to maintain the column in the loading zone. The evolution from 40 to 30 to 20 Nm^3/h was associated to the respective packing RSR1, Hiflow25 and RSR0.5 (metal). Characteristics of the packings are given in Table 1. The results obtain with this anisotropic configuration, with the packing properties being modified along the packing height according to the flowrate reduction by implementing layers of different unstructured packing materials, are presented in Figure 11 (b). It represents an arrangement of the packing with three layers placed on top of each other. The results show that for this configuration, the proposed packing evolution is able to maintain the gas velocity in the loading zone. Consequently, $\beta_G a_{Ph}$ is not reduced while the gas flows through the packing. It is

even higher ending at 1.54 s^{-1}. This type of evolutive packing could be beneficial for the upgrading process as it can reduce the size of the column with a higher (or at least stable) $\beta_G a_{Ph}$.

3.5 Energy analysis

The energy consumption is the final key parameter for the evaluation of upgrading processes. Associated to the methane recovery ratio, it provides an energy yield of the installation that can finally describe the energy production in the form of an energy return on investment.

The power requirements of the main devices are presented in Table 7. Experimental measurements of the electrical consumption were conducted for experiment 31 (at 30 Nm^3/h of biogas flowrate, with a water flowrate of 8 m^3/h, an absorption pressure of 9.7 bars and a vacuum pressure of 0.33 bar) and 35 (at 20 Nm^3/h of biogas flowrate, with a water flowrate of 6 m^3/h, an absorption pressure of 10.0 bars and a vacuum pressure of 0.2 bar). An electricity meter was used to evaluate the electrical consumption for 2 hours during these experiments. The electrical need was around 25 kW for experiment 31 and 16.6 kW for experiment 35. In each case, the normalized consumption related to the raw biogas treated is around 0.8 kWh/Nm^3. This value is higher than those encountered in the literature, usually comprised between 0.2 and 0.4 kWh/Nm^3. This is because the device is not optimized at all in terms of energy efficiency. Five points of improvement that can be easily implemented are discussed in the following:

- First, the process container was implemented at a certain distance from the digester for spatial layout and therefore the compressor has to suck the gas out from the digester on a certain distance leading to a vacuum at the inlet of the compressor. This leads to a limitation of the flowrate to 30 Nm^3/h when the frequency was 50 Hz even though it is supposed to reach 78 Nm^3/h for this compressor. A closer disposition should lead to lower consumption.
- Also, two pumps are used to circulate the water, one from the vacuum vessel to the water storage and one from the water storage to the column. Energy consumption could be reduced by using a single hydraulic pump and gathering the water storage and the vacuum vessel in a single vacuum tank.
- The vacuum pump is not frequency driven and depending on the gas that has to be evacuated, adjusting the frequency could help to reduce the energy consumption.
- The results demonstrate that the temperature has not much effect on the performances, and therefore the energy for refrigeration could be avoided.

- Finally, the blower fan that is used to renew and extract the air from the container to prevent an explosive atmosphere in case of a leak could be avoided for an industrial case.

Table 7: Motor power of the main electrical devices.

Device	Motor power (kW)
Pump 1	4
Pump 2	2.2
Vacuum Pump	2.2
Compressor	7.5
Water refrigeration	5
Blower fan	1.1
Total	21.9

Considering all these improvements, the power requirement (in kW) could be evaluated with Equation (6) for the pump (ξ_{pump}), Equation (7) for the compressor (ξ_{comp}), and Equation (8) for the vacuum pump (ξ_{vac}) [40,41]. The total power requirement ξ_{el} (in kW) is calculated as $\xi_{el} = \xi_{pump} + \xi_{comp} + \xi_{vac}$.

$$\xi_{pump} = \frac{\mathrm{Q}_0 \cdot (P_1 - P_5)}{\eta_{pump} \cdot 1000} \quad (6)$$

$$\xi_{comp} = \frac{0.371 \cdot T \cdot \gamma \cdot G_v}{(\gamma - 1) \cdot \eta_{comp}} \left[\left(\frac{P_1}{P_{Atm}} \right)^{1-\frac{1}{\gamma}} - 1 \right] \quad (7)$$

$$\xi_{vac} = 3.7 \cdot 10^{-5} \cdot 1.2 \cdot \mathrm{Q}_3 \cdot (P_{Atm} - P_5) \cdot 750 \quad (8)$$

η refers to the power device yield taken at 0.6 for the pump and 0.8 for the compressor. γ is the Laplace coefficient taken at 1.35.

The conditions used in experiments 35 are investigated as gas injection standards were achieved (over 97 % in methane). It is supposed that the recirculation of the GLCC does not affect E_{CO_2} and $R_{CH_4}^{col}$, just as the composition in the digester. An overconsumption is therefore considered to upgrade the 5.5 Nm^3/h of gas recirculated from the GLCC. The calculated energy consumptions are given in Table 8. The total energy consumption related to the raw biogas flow is 0.3 kWh/Nm^3 without the GLCC and 0.38 kWh/Nm^3 with the GLCC.

The energy efficiency of the biogas upgrading can be expressed as presented in Equation (9).

$$Eff = \frac{\xi_{biomethane}}{\xi_{biogas} + \xi_{el}} \quad (9)$$

Table 8: Energy consumption and energy efficiency of the HPWS with and without the GLCC.

Device	Without GLCC	With GLCC
ξ_{pump}	2.7	3.47
ξ_{comp}	2.4	3.08
ξ_{vac}	0.7	0.9
ξ_{el}	5.8	7.45
Eff	0.71	0.91

These results highlight that the energy consumption associated to the vacuum is not significant compared to the pump and the compressor (around 12 % of the total). The rough vacuum implemented is therefore of significant value as it improves the methane purity by far. Also, despite the GLCC requirement of an electrical overconsumption, it is more valuable for the energy efficiency and the methane recovery.

4 Conclusions

In this work, a full-scale biogas upgrading process was successfully set-up on a small-scale anaerobic digester. It allows to complete the literature with 36 experimental measures in very different configurations in terms of water flowrate, absorption pressure, intermediate pressure, water regeneration, temperature, and packing height variations. The process is stable in time and the repeatability of the measures was successfully evaluated.

Results show that the water temperature has very little influence on the process performances in the range of 288 to 309 K, as even if cold temperature enhances absorption, it reduces the desorption efficiency. Absorption pressure increases the methane purity, but also the gas leaks. A convenient pressure should be implemented to obtain the targeted purity without detrimental methane leaks. However, methane leaks can be mitigated by the recirculation at intermediate pressure. The water flowrate might be the adjustable variable of the process. The results show that once the maximal capacity of absorption is reach, an excessive flowrate leads to a great loss of methane. But before this turning point, an increase of the flowrate allows to enhance the methane purity without additional methane loss.

The influence of the regeneration of the water under rough vacuum was successfully evaluated. Experiments show that increasing the vacuum is associated to a higher methane purity, as the water is efficiently degassed. To the

authors' knowledge, this is the first experimental validation of the benefit of vacuum regeneration on an actual biogas flow. Moreover, a slight increase of the packing height was performed, from 2.65 to 3.35 m (height-to-diameter ratio from 8.8 to 11.2) with an evolutive packing (three layers). This increase allows to reach more than 97 % of methane purity in the upgraded biomethane, suitable for gas grid injection. Billet-Schultes correlations were used to highlight that as the volumetric gas flow decrease along the packing due to absorption, mass transfer efficiency also decreases for a given packing. An anisotropic configuration of the packing should therefore be proposed for biogas upgrading.

Finally, the energetical consumption was evaluated. Due to the configuration, measured consumptions were around 0.8 kWh/Nm^3, but with a more adapted lay out, 0.3 kWh/Nm^3 are expected. Gas recirculation due to the intermediate desorption increases this value to 0.38 kWh/Nm^3, that is in the range given in the literature. Gas recirculation enhances the energy efficiency from 0.71 to 0.91.

This work demonstrates the feasibility of biogas upgrading with HPWS on small-scale anaerobic digestion with performances suitable for gas grid injection in an economical configuration.

Acknowledgments

The authors are very grateful to the French Environment and Energy Management Agency (ADEME) for the funding support provided within the EPUROGAZ grant.

References

[1] IPCC, Summary for Policymakers — Global Warming of 1.5 °C, (2018).

[2] N. Scarlat, J.-F. Dallemand, F. Fahl, Biogas: Developments and perspectives in Europe, Renewable Energy. 129 (2018) 457–472. https://doi.org/10.1016/j.renene.2018.03.006.

[3] U. Brémond, A. Bertrandias, J.-P. Steyer, N. Bernet, H. Carrere, A vision of European biogas sector development towards 2030: Trends and challenges, Journal of Cleaner Production. 287 (2021) 125065. https://doi.org/10.1016/j.jclepro.2020.125065.

[4] S. O'Connor, E. Ehimen, S.C. Pillai, A. Black, D. Tormey, J. Bartlett, Biogas production from small-scale anaerobic digestion plants on European farms, Renewable and Sustainable Energy Reviews. 139 (2021) 110580. https://doi.org/10.1016/j.rser.2020.110580.

[5] S.P. Lohani, B. Dhungana, H. Horn, D. Khatiwada, Small-scale biogas technology and clean cooking fuel: Assessing the potential and links with SDGs in low-income countries – A case study of Nepal, Sustainable Energy Technologies and Assessments. 46 (2021) 101301. https://doi.org/10.1016/j.seta.2021.101301.

[6] A. Baccioli, M. Antonelli, S. Frigo, U. Desideri, G. Pasini, Small scale bio-LNG plant: Comparison of different biogas upgrading techniques, Applied Energy. 217 (2018) 328–335. https://doi.org/10.1016/j.apenergy.2018.02.149.

[7] L. Yang, X. Ge, C. Wan, F. Yu, Y. Li, Progress and perspectives in converting biogas to transportation fuels, Renewable and Sustainable Energy Reviews. 40 (2014) 1133–1152. https://doi.org/10.1016/j.rser.2014.08.008.

[8] Q. Sun, H. Li, J. Yan, L. Liu, Z. Yu, X. Yu, Selection of appropriate biogas upgrading technology-a review of biogas cleaning, upgrading and utilisation, Renewable and Sustainable Energy Reviews. 51 (2015) 521–532. https://doi.org/10.1016/j.rser.2015.06.029.

[9] I. Angelidaki, L. Treu, P. Tsapekos, G. Luo, S. Campanaro, H. Wenzel, P.G. Kougias, Biogas upgrading and utilization: Current status and perspectives, Biotechnology Advances. 36 (2018) 452–466. https://doi.org/10.1016/j.biotechadv.2018.01.011.

[10] S. Sarker, J.J. Lamb, D.R. Hjelme, K.M. Lien, Overview of recent progress towards in-situ biogas upgradation techniques, Fuel. 226 (2018) 686–697. https://doi.org/10.1016/j.fuel.2018.04.021.

[11] S. Fu, I. Angelidaki, Y. Zhang, In situ Biogas Upgrading by CO2-to-CH4 Bioconversion, Trends in Biotechnology. 39 (2021) 336–347. https://doi.org/10.1016/j.tibtech.2020.08.006.

[12] J. Zhao, Y. Li, R. Dong, Recent progress towards in-situ biogas upgrading technologies, Science of The Total Environment. 800 (2021) 149667. https://doi.org/10.1016/j.scitotenv.2021.149667.

[13] L. Rachbauer, G. Voitl, G. Bochmann, W. Fuchs, Biological biogas upgrading capacity of a hydrogenotrophic community in a trickle-bed reactor, Applied Energy. 180 (2016) 483–490. https://doi.org/10.1016/j.apenergy.2016.07.109.

[14] S. Cheng, D. Xing, D.F. Call, B.E. Logan, Direct Biological Conversion of Electrical Current into Methane by Electromethanogenesis, Environ. Sci. Technol. 43 (2009) 3953–3958. https://doi.org/10.1021/es803531g.

[15] E. Mulu, M.M. M'Arimi, R.C. Ramkat, A.C. Mecha, Potential of wood ash in purification of biogas, Energy for Sustainable Development. 65 (2021) 45–52. https://doi.org/10.1016/j.esd.2021.09.009.

[16] C. Moya, R. Santiago, D. Hospital-Benito, J. Lemus, J. Palomar, Design of biogas upgrading processes based on ionic liquids, Chemical Engineering Journal. 428 (2022) 132103. https://doi.org/10.1016/j.cej.2021.132103.

[17] A. Chidambaram, D.H. Le, J.A.R. Navarro, K.C. Stylianou, Robust metal-organic frameworks for dry and wet biogas upgrading, Applied Materials Today. 22 (2021) 100933. https://doi.org/10.1016/j.apmt.2020.100933.

[18] C. Yan, L. Zhu, Y. Wang, Photosynthetic CO2 uptake by microalgae for biogas upgrading and simultaneously biogas slurry decontamination by using of microalgae photobioreactor under various light wavelengths, light intensities, and photoperiods, Applied Energy. 178 (2016) 9–18. https://doi.org/10.1016/j.apenergy.2016.06.012.

[19] L. Zhu, C. Yan, Z. Li, Microalgal cultivation with biogas slurry for biofuel production, Bioresource Technology. 220 (2016) 629–636. https://doi.org/10.1016/j.biortech.2016.08.111.

[20] C. Yan, R. Muñoz, L. Zhu, Y. Wang, The effects of various LED (light emitting diode) lighting strategies on simultaneous biogas upgrading and biogas slurry nutrient reduction by using of microalgae Chlorella sp., Energy. 106 (2016) 554–561. https://doi.org/10.1016/j.energy.2016.03.033.

[21] L. Laguillaumie, Y. Rafrafi, E. Moya-Leclair, D. Delagnes, S. Dubos, M. Spérandio, E. Paul, C. Dumas, Stability of ex situ biological methanation of H2/CO2 with a mixed microbial culture in a pilot scale bubble column reactor, Bioresource Technology. 354 (2022) 127180. https://doi.org/10.1016/j.biortech.2022.127180.

[22] R. Kapoor, P. Ghosh, V.K. Vijay, Chapter 4 - Factors affecting CO2 and CH4 separation during biogas upgrading in a water scrubbing process, in: N. Aryal, L.D. Mørck Ottosen, M.V. Wegener Kofoed, D. Pant (Eds.), Emerging Technologies and Biological Systems for Biogas Upgrading, Academic Press, 2021: pp. 73–91. https://doi.org/10.1016/B978-0-12-822808-1.00004-0.

[23] Å. Tynell, G. Börjesson, M. Persson, Microbial growth on pall rings: A problem when upgrading biogas with the water-wash absorption technique, Appl Biochem Biotechnol. 141 (2007) 299–319. https://doi.org/10.1007/BF02729069.

[24] P. Cozma, W. Wukovits, I. Mămăligă, A. Friedl, M. Gavrilescu, Modeling and simulation of high pressure water scrubbing technology applied for biogas upgrading, Clean Techn Environ Policy. 17 (2015) 373–391. https://doi.org/10.1007/s10098-014-0787-7.

[25] S. Rasi, J. Läntelä, A. Veijanen, J. Rintala, Landfill gas upgrading with countercurrent water wash, Waste Management. 28 (2008) 1528–1534. https://doi.org/10.1016/j.wasman.2007.03.032.

[26] J. Läntelä, S. Rasi, J. Lehtinen, J. Rintala, Landfill gas upgrading with pilot-scale water scrubber: Performance assessment with absorption water recycling, Applied Energy. 92 (2012) 307–314. https://doi.org/10.1016/j.apenergy.2011.10.011.

[27] R. Kapoor, P.M.V. Subbarao, V.K. Vijay, G. Shah, S. Sahota, D. Singh, M. Verma, Factors affecting methane loss from a water scrubbing based biogas upgrading system, Applied Energy. 208 (2017) 1379–1388. https://doi.org/10.1016/j.apenergy.2017.09.017.

[28] R. Kapoor, P.M.V. Subbarao, V.K. Vijay, Integration of flash vessel in water scrubbing biogas upgrading system for maximum methane recovery, Bioresource Technology Reports. 7 (2019) 100251. https://doi.org/10.1016/j.biteb.2019.100251.

[29] D. Benizri, N. Dietrich, P. Labeyrie, G. Hébrard, A compact, economic scrubber to improve farm biogas upgrading systems, Separation and Purification Technology. 219 (2019) 169–179. https://doi.org/10.1016/j.seppur.2019.02.054.

[30] E. Wantz, D. Benizri, N. Dietrich, G. Hébrard, Rate-based modeling approach for High Pressure Water Scrubbing with unsteady gas flowrate and multicomponent absorption applied to biogas upgrading, Applied Energy. 312 (2022) 118754. https://doi.org/10.1016/j.apenergy.2022.118754.

[31] F. Jin, H. Xu, D. Hua, L. Chen, Y. Li, Y. Zhao, B. Zuo, Enhancement of CO2 desorption using ultrasound and vacuum in water scrubbing biogas upgrading system, Korean J. Chem. Eng. 38 (2021) 129–134. https://doi.org/10.1007/s11814-020-0686-z.

[32] K. Gładyszewski, K. Groβ, A. Bieberle, M. Schubert, M. Hild, A. Górak, M. Skiborowski, Evaluation of performance improvements through application of anisotropic foam packings in rotating packed beds, Chemical Engineering Science. 230 (2021) 116176. https://doi.org/10.1016/j.ces.2020.116176.

[33] R. Hreiz, C. Gentric, N. Midoux, R. Lainé, D. Fünfschilling, Hydrodynamics and velocity measurements in gas–liquid swirling flows in cylindrical cyclones, Chemical Engineering Research and Design. 92 (2014) 2231–2246. https://doi.org/10.1016/j.cherd.2014.02.029.

[34] S. Wang, L. Gomez, R. Mohan, O. Shoham, G. Kouba, J. Marrelli, The State-of-the-Art of Gas-Liquid Cylindrical Cyclone Control Technology: From Laboratory to Field, Journal of Energy Resources Technology. 132 (2010). https://doi.org/10.1115/1.4001900.

[35] D. Benizri, N. Dietrich, P. Labeyrie, G. Hébrard, A compact, economic scrubber to improve farm biogas upgrading systems, Separation and Purification Technology. 219 (2019) 169–179. https://doi.org/10.1016/j.seppur.2019.02.054.

[36] S. Rohani, Y. Wu, Chapter 1 - Introduction, in: S. Rohani (Ed.), Coulson and Richardson's Chemical Engineering (Fourth Edition), Butterworth-Heinemann, 2017: pp. 1–16. https://doi.org/10.1016/B978-0-08-101095-2.00001-1.

[37] M. Götz, W. Köppel, R. Reimert, F. Graf, Optimierungspotenzial von Wäschen zur Biogasaufbereitung. Teil 1 - Physikalische Wäschen, Chemie Ingenieur Technik. 83 (2011) 858–866. https://doi.org/10.1002/cite.201000211.

[38] P. Rotunno, A. Lanzini, P. Leone, Energy and economic analysis of a water scrubbing based biogas upgrading process for biomethane injection into the gas grid or use as transportation fuel, Renewable Energy. 102 (2017) 417–432. https://doi.org/10.1016/j.renene.2016.10.062.

[39] R. Billet, M. Schultes, Prediction of Mass Transfer Columns with Dumped and Arranged Packings: Updated Summary of the Calculation Method of Billet and Schultes, Chemical Engineering Research and Design. 77 (1999) 498–504. https://doi.org/10.1205/026387699526520.

[40] W.L. McCabe, J.C. Smith, P. Harriott, Unit Operations of Chemical Engineering, McGraw-Hill, 1993.

[41] D. Hoffman, B. Singh, J. Thomas, Handbook of Vacuum Science and Technology, Academic Press, Elsevier, 1998.

Nomenclature

Abbreviations

Eff	Energy efficiency
GLCC	Gas Liquid Cylindrical Cyclone
GCV	Gas Control Valve
HPWS	High Pressure Water Scrubber
LCV	Liquid Control Valve
$Nm^3.h^{-1}$	Gas Volumetric flowrate at standard conditions (273.15 K and one atmosphere)
PID	Proportional Integral Derivative
RSR	Raschig Super Ring

General

A_i	Analysis point
a^*	Wetted surface area ($m^2.m^{-3}$)
d_p	Diameter of a packing unit (m)
$E_{CO_2}^{(app)}$	(apparent) Carbon dioxide elimination rate (-)
G	Gas mass flowrate ($kg.s^{-1}$)
L	Liquid mass flowrate ($kg.s^{-1}$)
N	Quantity of packing pieces per cubic meter
P	Absolute Pressure (bar)
$Q_{0,1,2,3,4}$	Flowrate of the water (m^3/h), bio-CH_4, GLCC, bioCO_2 and biogas (Nm^3/h)
$R_{CH_4}^{(col)[glob]}$	(column) [global] Methane Recovery ratio (-)

$T_{1(2)}$	(Water) Gas Temperature (K)
u_G	Gas velocity (m.s^{-1})
x	Molar fraction of solute in liquid (mol.mol^{-1})
y	Molar fraction of solute in gas (mol.mol^{-1})
$\bar{y}$	Normalized molar fraction (mol.mol^{-1})

Subscripts and Superscripts

comp	Refers to the compressor
Fl	Flooding
G	Refers to the gas phase
L	Refers to the liquid phase
Lo	Loading
M	Mass
mod	Modeled
pump	Refers to the hydraulic pump
vac	Refers to the vacuum pump

Greek Letter

$\beta_G a_{Ph}$	Volumetric Mass Transfer (s^{-1})
γ	Laplace coefficient (-)
ε_G	Packing Void ratio (-)
η	Power device yield (-)
μ	Viscosity (Pa.s)
ξ	Energy consumption (kWh.Nm^{-3})
ρ	Volumetric mass density (kg.m^{-3})